NRC Research Press

ARTICLE

Design-based regression estimation of net change for forest inventories

Alexander Massey and Daniel Mandallaz

Abstract: A simple design-based approach to estimating net change of a forest attribute such as timber volume is to observe the change directly on the plot level and then make that the response variable of interest using established estimation techniques such as multiphase regression estimators. This direct approach is only possible for inventories with permanent plots and is constrained to estimating net change over time periods matching the duration of the remeasurement cycle. Indirect estimation involves applying one of the aforementioned techniques to estimate the state at two time points and taking their difference. Indirect methods, although less common, are not necessarily constrained to permanent plots and can estimate net change over any desired time span for annual designs. This article compares design-based direct and indirect regression estimators under the Monte Carlo approach and illustrates their performances with data from the Swiss National Forest Inventory. The major finding is that direct estimation should be preferred whenever change is observable directly on the plot level but that multiphase indirect estimation can still improve precision when direct estimation is not possible such as for inventories employing only temporary plots.

Key words: design based, Monte Carlo approach, three-phase regression estimation, direct and indirect net change estimation, forest inventory.

Résumé : Une méthode simple pour estimer la variation nette d'un attribut comme le matériel sur pied est d'observer directement cette variation au niveau de la placette, puis de s'en servir comme variable cible dans le cadre d'estimateurs multiphases. Cette approche directe n'est possible qu'avec des placettes permanentes et où l'intervalle entre deux mesures correspond au cycle complet d'inventaire. L'approche indirecte consiste à estimer l'état de l'attribut en deux instants donnés et de prendre leur différence comme estimateur de la variation nette. Cette technique est aussi applicable avec des placettes temporaires et permet dans le cadre d'inventaires annuels d'estimer la variation sur une période arbitraire. Cet article décrit les méthodes directes et indirectes dans le cadre d'estimateurs par régression et de l'inférence sous le plan de sondage dans le formalisme Monte-Carlo. L'article illustre les performances de plusieurs estimateurs avec des données de l'inventaire Forestier National Suisse. Le résultat principal est que la méthode directe est préférable pour autant qu'elle soit possible, dans le cas contraire la précision de l'estimation peut être néanmoins améliorée en utilisant les estimateurs par régression multiphases.

Mots-clés : inférence sous le plan de sondage, formalisme Monte-Carlo, estimateur par régression à trois phases, estimation directe et indirecte de la variation nette, inventaire forestier.

1. Introduction

In 2009, the Swiss National Forest Inventory (NFI) changed from a periodic design, conducted approximately every 10 years based on two-phase sampling with manually interpreted aerial stereophotographs on a 0.5 km × 0.5 km grid in the first phase and terrestrial plots on a subgrid of $\sqrt{2}$ km × $\sqrt{2}$ km, to an annual design, where one-ninth of the permanent terrestrial plots were selected uniformly across the country to be evaluated every year. This change, which was primarily motivated by a desire to produce estimates continuously over time, as well as by the logistic benefits associated with a regular inventory schedule, results in a loss in precision due to the reduction of available sample size for a given time point t_k. Consequently, new statistical procedures are needed that efficiently incorporate remote sensing information to estimate the state of the forest at a given time, i.e., the spatial mean of over-bark bole volume at time period t_k, denoted $\overline{Y}(t_k)$, and also its change over time, i.e., $\overline{Y}(t_2) - \overline{Y}(t_1)$. The estimation of the state for the Swiss NFI has been addressed via the proposal of a three-phase regression estimator with remote sensing data at the first phase, updates of the terrestrial plots (with growth models) at the second phase, and the current annual inventory at the third phase (Massey et al. (2014)). However, the estimation of net change remains a challenge under the annual design, and the estimation of the classical growth components (survivor growth, in growth, on growth, nongrowth, and depletion, see Mandallaz (2008), chapter 11) even more so, particularly if one wants to use the two-stage procedure at the plot level (which yields better estimates of the bole volume).

Many studies have demonstrated that model-assisted estimation with aerial remote sensing data such as LiDAR can dramatically increase the precision of net change estimates (Næsset et al. (2013); Skowronski et al. (2014)). Literature concerning model-assisted methods for enhancing estimation under an annual design is currently scarce. Annual designs for NFIs already exist in Finland (Tomppo (2006)), Sweden (Barklund (2009)), France (Vidal et al. (2005)), and the United States (Schreuder et al. (2000)). However, it should be noted that of these countries, only the US Forest Inventory Analysis (FIA) uses only permanent plots as the Swiss NFI does. The French NFI uses only temporary plots, whereas

Received 3 July 2015. Accepted 22 September 2015.

A. Massey. WSL, Swiss Federal Research Institute, CH 8903 Birmensdorf, Switzerland.
D. Mandallaz. Chair of Land Use Engineering, ETH Zurich, CH 8092 Zurich, Switzerland.
Corresponding author: Alexander Massey (e-mail: alexander.massey@wsl.ch).

Published at www.nrcresearchpress.com/cjfr on 29 September 2015.

Sweden and Finland use a combination of both. Finland and Sweden have already put into place plot-updating and model-assisted estimation procedures for NFIs, and other countries can be expected to follow suit.

The most common approach to estimating the change when permanent plots are present is to observe the change directly on the plot level and then treat that as the variable of interest. In the presence of annual designs, one is thus able to estimate net change directly on a continuous basis but only across time spans, denoted $t_2 - t_1$, that are multiples of the time it takes to complete a full cycle of the annual inventory. This approach is flexible and seamlessly allows for the implementation of model-assisted techniques such as the use of two- and three-phase regression estimators to mitigate this loss of precision due to reduced sample size while remaining design unbiased. However, if one wants to circumvent the drawback of only being able to make estimates for predetermined time spans, one must estimate net change indirectly by taking the difference between estimates of the state of the forest at two distinct time points, which still leads to an unbiased estimate in the design-based sense. Although it is generally thought that direct change estimation leads to lower variances when compared with indirect estimation over the same observable time span (Skowronski et al. (2014)), this notion has recently been challenged by McRoberts et al. (2015) for two-phase regression estimation. The paper presented here explores the utility of design-based direct and indirect net change estimation in the context to the Swiss NFI and expands the methodology to three-phase regression estimators. Furthermore, it provides suggestions for indirect estimators under annual designs for time spans where direct estimation is not possible.

2. The sampling design

We want to estimate the net change between times t_1 and t_2 of the spatial mean of the timber volume densities over the permanent forested area F (new forested area and new nonforested area are excluded from this analysis). We have a well-defined population P of trees $i \in 1, 2, \ldots, N(t_k)$ in forest F, and for every tree, we have a response variable Y_i, which, in this case, is the individual tree's over-bark bole volume. The spatial mean at time t_k measured in cubic meters per hectare is denoted $\bar{Y}(t_k) := [1/\lambda(F)]\sum_{i=1}^{N(t_k)} Y_i(t_k)$, for $k = 1, 2$, where $\lambda(F)$ is the surface area of F, and the parameter of interest is $\Delta_{\bar{Y}}(t_1, t_2) := \bar{Y}(t_2) - \bar{Y}(t_1)$.

We propose the following three-phase setup. The first phase is presumably derived from remote sensing data and consists of a large sample s_1 of n_1 points, where $x \in F$ are assumed to be distributed uniformly and independently in F whose information is contained in row vector $\boldsymbol{Z}^{(1)t}(x)$. The second phase $s_2 \subset s_1$ of n_2 points is drawn by simple random sampling (SRS) without replacement from s_1 and comprises information obtained from terrestrial plots from the full cycle of the annual design (usually some growth updated form of the previous plot volume measurement at x). Thus auxiliary information for every $x \in s_2$ is contained in row vector $\boldsymbol{Z}^t(x) = (\boldsymbol{Z}^{(1)t}(x), \boldsymbol{Z}^{(2)t}(x))$, where $\boldsymbol{Z}^{(2)t}(x)$ represents the terrestrially acquired or computationally intensive remote sensing information (Mandallaz (2014)). The third-phase sample at time t_k is denoted by s_{3k} with n_{3k} points drawn by SRS without replacement from s_2. The third phase yields the ground truth under the annual design of the local densities $Y(t_k, x)$ at time t_k, where $k = 1, 2$.

Although most NFIs typically use systematic sampling schemes with a random start, treating systematic samples as uniformly random samples is rarely a problem for point estimates that remain asymptotically unbiased. In practice, the variance is usually overestimated, particularly for small area estimation (see Mandallaz (2008), chapter 7). Furthermore, because we are in the design-based framework, the local density estimate $Y(t_k, x)$ is assumed to be error free given x at time t_k and the random selection x is uniform in F. We are using the Monte Carlo approach in the design-based setup, where the relation $\mathbb{E}_x(Y(t_k, x)) = [1/\lambda(F)]\int_F Y(t_k, x)dx = [1/\lambda(F)]\sum_{i=1}^{N} Y_i(t_k) = \bar{Y}(t_k)$ holds for both fixed-radius or variable-radius (angle count) sampling of trees, which requires that our sample selection of x is uniformly and independently drawn in F.

We now consider two situations concerning s_{31} and s_{32}. Let L be the complete cycle length of the annual inventory measured in vegetative periods (i.e., the measurement of time excludes months that do not coincide with the growing season). The first situation is when $s_{31} = s_{32}$, i.e., $t_2 - t_1$ equals a multiple of L. The second situation occurs when $t_2 - t_1$ is not a multiple of L such that $s_{31} \cap s_{32} = \emptyset$ (for simplicity, we ignore scenarios where s_{31} and s_{32} only partially overlap, which can occur when t_k represent groupings of multiple years).

If $s_{31} = s_{32}$ and we neglect the auxiliary information obtained from s_1 and s_2, the direct and indirect net change estimators become mathematically equivalent. Denoting $Y_\Delta(x) := Y(t_2, x) - Y(t_1, x)$, $n_3 := n_{31} = n_{32}$, and $s_3 := s_{31} = s_{32}$

$$(1) \qquad \hat{\Delta}_{\mathrm{dir,1p}}(t_1, t_2) := \frac{1}{n_3}\sum_{x\in s_3} Y_\Delta(x)$$

$$(2) \qquad \hat{\Delta}_{\mathrm{dir,1p}}(t_1, t_2) = \frac{1}{n_{32}}\sum_{x\in s_{32}} Y(t_2, x) - \frac{1}{n_{31}}\sum_{x\in s_{31}} Y(t_1, x) =: \hat{\Delta}_{\mathrm{indir,1p}}(t_1, t_2)$$

are unbiased estimators of the parameter $\Delta_{\bar{Y}}(t_1, t_2)$ with unbiased variance estimator

$$(3) \qquad \hat{\mathbb{V}}(\hat{\Delta}_{\mathrm{dir,1p}}(t_1, t_2)) = \frac{1}{n_3}\frac{1}{n_3 - 1}\sum_{x\in s_3}(Y_\Delta(x) - \bar{Y}_{\Delta,s_3})^2$$

where $\bar{Y}_{\Delta,s_3} := (1/n_3)\sum_{x\in s_3} Y_\Delta(x)$ for notational convenience. In our notation, the subscript 1p indicates that estimator is for one phase, and subscripts dir or indir indicate whether it is direct or indirect, respectively.

If $s_{31} \cap s_{32} = \emptyset$, then $Y_\Delta(x)$ is unobservable and only indirect calculation is possible using eq. 2, which is still design unbiased for the point estimate. However, the variance of the change will be the sum of the variances for the states at t_1 and t_2

$$(4) \qquad \hat{\mathbb{V}}(\hat{\Delta}_{\bar{Y}_\Delta}(t_1, t_2)) = \frac{1}{n_{32}}\frac{1}{n_{32} - 1}\sum_{x\in s_{32}}(Y(t_2, x) - \bar{Y}_{s_{32}})^2 + \frac{1}{n_{31}}\frac{1}{n_{31} - 1}\sum_{x\in s_{31}}(Y(t_1, x) - \bar{Y}_{s_{31}})^2$$

where $\bar{Y}_{s_{3k}} = (1/n_{3k})\sum_{x\in s_{3k}} Y(t_k, x)$ for $k = 1, 2$. The variance in eq. 4 is likely to be unacceptably high because of the independence between s_{31} and s_{32}. We expect to obtain more precise design-unbiased estimators of $\Delta_{\bar{Y}}(t_1, t_2)$ by incorporating the information from the auxiliary vectors $\boldsymbol{Z}^{(1)t}(x)$ and $\boldsymbol{Z}^t(x)$ using model-assisted estimation.

3. Model-assisted estimation of net change

3.1. The external model approach

All estimators presented here are based on generalized difference (GD) estimators derived under the external model approach. Difference estimators were proposed by Särndal et al. (2003) (section 9.7) for linear models in the finite population context where one has exhaustive auxiliary information and then adapted for the Monte Carlo infinite population approach by Mandallaz (2008, 2013*a*, 2014). The three-phase version is defined as

$$\hat{Y}_{\mathrm{GD,3p}} = \frac{1}{n_1}\sum_{x\in s_1}\hat{Y}^{(1)}(x) + \frac{1}{n_2}\sum_{x\in s_2}(\hat{Y}(x) - \hat{Y}^{(1)}(x)) + \frac{1}{n_3}\sum_{x\in s_3}(Y(x) - \hat{Y}(x)) \quad (5)$$

where $\hat{Y}^{(1)}(x)$ and $\hat{Y}(x)$ are model predictions applied to $\boldsymbol{Z}^{(1)t}(x)$ and $\boldsymbol{Z}^{t}(x)$, respectively. The associated analytical variance is

$$\mathbb{V}(\hat{Y}_{\mathrm{GD,3p}}) = \frac{1}{n_1}\mathbb{V}(Y(x)) + \left(1 - \frac{n_2}{n_1}\right)\frac{1}{n_2}\mathbb{V}(R^{(1)}(x)) + \left(1 - \frac{n_3}{n_2}\right)\frac{1}{n_3}\mathbb{V}(R(x)) \quad (6)$$

where $R^{(1)}(x) \coloneqq Y(x) - \hat{Y}^{(1)}(x)$ and $R(x) \coloneqq Y(x) - \hat{Y}(x)$. Equation 6 can be estimated using sample copies of the variance terms over s_3, s_1, and s_2, respectively. For notational consistency, we remove one of the phases by setting $s_1 = s_2$ so that s_2 now represents the first phase. In some ways, this notational convention is unfortunate, but it allows for s_3 to always represent the final phase, consisting of the ground truth. The two-phase version is defined as

$$\hat{Y}_{\mathrm{GD,2p}} = \frac{1}{n_2}\sum_{x\in s_2}\hat{Y}(x) + \frac{1}{n_3}\sum_{x\in s_3}(Y(x) - \hat{Y}(x)) \quad (7)$$

with variance

$$\mathbb{V}(\hat{Y}_{\mathrm{GD,2p}}) = \frac{1}{n_2}\mathbb{V}(Y(x)) + \left(1 - \frac{n_3}{n_2}\right)\frac{1}{n_3}\mathbb{V}(R(x)) \quad (8)$$

The estimators eqs. 5 and 7 and the sample copy estimators for eqs. 6 and 8 remain exactly design unbiased regardless of what models (linear, nonparametric, nearest neighbor, etc.) are specified to generate the predictions, provided that we work under the external model assumption. A model is called external if the training set used to fit it does not depend on the current inventory sample realization. This ensures that $\hat{Y}^{(1)}(x)$ (likewise $\hat{Y}(x)$) remain i.i.d. across all $x \in s_1$, s_2, and s_3 (notice that there are no potentially complicated design-based covariance terms in eqs. 6 or 8). In practice, of course, true external models are rarely, if ever, used because most practitioners use s_3 as a training set, thus making the model internal. Applying formulas derived under the external model assumption to internal models may still be asymptotically acceptable (as is the case for linear models), but the adequacy of this approach is questionable for other model types such as k nearest neighbours (kNN) (see Massey and Mandallaz (2015)). For simplicity, all analytical estimators proposed here are derived under the external model approach, and the resulting external variances are compared with the bootstrap.

3.2. Direct estimation

For direct estimation of change, $Y_\Delta(x)$ must be observable. Thus, we are in a permanent plot setup and, for simplicity, assume that $s_{31} = s_{32}$. Only point estimators and variance estimators are given here, but the interested reader is referred to Mandallaz (2008), p. 80 and appendix B, for mathematical details concerning the derivations. The direct estimators are obtained simply by plugging $Y_\Delta(x)$, $\hat{Y}^{(1)}_\Delta(x)$, and $\hat{Y}_\Delta(x)$ into the difference estimator for $Y(x)$, $\hat{Y}^{(1)}(x)$, and $\hat{Y}(x)$, respectively, and likewise for the residuals. The three- and two-phase direct estimators are thus defined as follows:

$$\hat{\Delta}_{\mathrm{dir,3p}}(t_1, t_2) = \frac{1}{n_1}\sum_{x\in s_1}\hat{Y}^{(1)}_\Delta(x) + \frac{1}{n_2}\sum_{x\in s_2}\left(\hat{Y}_\Delta(x) - \hat{Y}^{(1)}_\Delta(x)\right) + \frac{1}{n_3}\sum_{x\in s_3}(Y_\Delta(x) - \hat{Y}_\Delta(x)) \quad (9)$$

$$\hat{\Delta}_{\mathrm{dir,2p}}(t_1, t_2) = \frac{1}{n_2}\sum_{x\in s_2}\hat{Y}_\Delta(x) + \frac{1}{n_3}\sum_{x\in s_3}(Y_\Delta(x) - \hat{Y}_\Delta(x)) \quad (10)$$

with corresponding variance estimators

$$\hat{\mathbb{V}}(\hat{\Delta}_{\mathrm{dir,3p}}(t_1, t_2)) = \frac{1}{n_1}\hat{\mathbb{V}}(Y_\Delta(x)) + \left(1 - \frac{n_2}{n_1}\right)\frac{1}{n_2}\hat{\mathbb{V}}(\hat{R}^{(1)}_\Delta(x)) + \left(1 - \frac{n_3}{n_2}\right)\frac{1}{n_3}\hat{\mathbb{V}}(\hat{R}_\Delta(x)) \quad (11)$$

$$\hat{\mathbb{V}}(\hat{\Delta}_{\mathrm{dir,2p}}(t_1, t_2)) = \frac{1}{n_2}\hat{\mathbb{V}}(Y_\Delta(x)) + \left(1 - \frac{n_3}{n_2}\right)\frac{1}{n_3}\hat{\mathbb{V}}(\hat{R}_\Delta(x)) \quad (12)$$

where on the right-hand side $\hat{\mathbb{V}}$ is defined as the sample variance in s_3.

$\hat{\Delta}_{\mathrm{dir,3p}}(t_1, t_2)$ and $\hat{\Delta}_{\mathrm{dir,2p}}(t_1, t_2)$ offer great flexibility when incorporating auxiliary information from different time points, as well as sources such as remote sensing and terrestrially acquired data. The auxiliary variables chosen to be represented in $\boldsymbol{Z}^t(x)$ only need to be chosen so that they predict the net change, $Y_\Delta(x)$, as efficiently as possible. From a strict mathematical point of view, it is irrelevant which explanatory variables are used, and it can well be the case that the relevant variables for the estimation of state are not all relevant for the estimation of change and vice versa. Practically, it would seem reasonable to include pairs of remote sensing measurements, e.g., for mean canopy height (MCH), representing both t_1 and t_2. However, if a linear model is used and MCH at t_1 and MCH at t_2 are included separately in $\boldsymbol{Z}^t(x)$, then separate coefficients will be fit for the pair. If only a single variable representing the difference in MCH at t_1 and t_2 is included, then only one coefficient is fit (see McRoberts et al. (2015) for details).

3.2.1. *Classical regression estimators*

Classical regression estimators are obtained by letting $\hat{Y}^{(1)}_\Delta(x) \coloneqq \boldsymbol{Z}^{(1)t}(x)\hat{\alpha}$ and $\hat{Y}_\Delta(x) \coloneqq \boldsymbol{Z}^t(x)\hat{\beta}$, where $\hat{\alpha}$ and $\hat{\beta}$ are simply the solutions to the normal equations when regressing $Y_\Delta(x)$ on $\boldsymbol{Z}^{(1)t}(x)$ and $Y_{\Delta(}x)$ on $\boldsymbol{Z}^t(x)$, respectively, for all $x \in s_3$. These classical regression estimators, as well as their variance estimators, are approximately design unbiased even when they are fit internally and treated as external. Depending on the mixture of categorical and continuous variables, as well as their potential interactions, special cases of the regression estimator arise such as poststratification and regression within stratification (see Massey et al. (2014) for an overview of special cases and Lüpke et al. (2012) for a detailed description of regression within stratification). It should be noted that, for linear models only, there exists another analytical variance estimator known as the g-weight variance estimator that better accounts for the effect of fitting a linear model internally through the use of first-order Taylor approximations. Although these estimators are known to possess better statistical properties than the variance estimators derived under the external approach, the g-weight version will not be discussed any further here, because there currently are no analogous versions for kNN (Massey and Mandallaz (2015)). However, details for the interested reader can be found in Mandallaz (2008, 2013*a*, 2014).

3.2.2. *Nonparametric regression estimators*

We obtain a nonparametric regression estimator by using s_3 as a reference set to produce the predictions for $\hat{Y}^{(1)}_\Delta(x)$ and $\hat{Y}_\Delta(x)$. Nonparametric kernel estimators such as the Nadaraya-Watson and kNN estimators are discussed in detail by Massey and Mandallaz (2015). There is some evidence that the kNN regression estimator can perform better than the classical regression estimator when the auxiliary variables lead to a lower goodness of fit, as defined by the R^2 (Haara and Kangas (2012)). The external variance estimators

obtained by eqs. 11 and 12 may be prone to underestimating the theoretical variance under moderate sample sizes, and a bootstrap routine is recommended (Massey and Mandallaz (2015)). The simplest way to implement such a bootstrap is to resample from s_1 using SRS with replacement, allowing n_2 and n_3 to be random in each bootstrap sample. Pseudo estimates are then computed by applying the desired estimator to each bootstrap sample. The sample variance of the pseudo estimates is the bootstrap variance estimate. To improve stability, tuning parameters such as the choice of k should be chosen based on the original sample only and held fixed across all bootstrap replications (Massey and Mandallaz (2015)).

3.2.3. *Advantages and drawbacks*

The main advantages of the direct change estimators presented are that their fits are optimized directly on the variable of interest. Moreover, at least for linear models, there exist reliable analytical variance estimators that facilitate the reproducibility of results. It should be noted that one often expects a slight underestimation when applying the external variance formulas to internal models. Intuitively, this is due to neglecting the effect of sampling variability on the fit.

The main drawback of the direct change estimation under annual designs is that there is dependency on the period of the remeasurement cycle, which is often not very flexible. For example, the Swiss NFI currently employs an annual design where approximately one-ninth of the plots are remeasured every year. Thus the remeasurement period will always be multiples of 9 years. Net change can, of course, be annualized by dividing by the length of the remeasurement period, but this implies a constant rate of change, which may not be realistic. If a net change estimate is desired over a period with a length different than the remeasurement period, then one has to extrapolate based on this linearization.

The main trouble area for direct change estimation is that the quality of the prediction for $Y_\Delta(x)$ is dependent on good synchronicity in the timing of the remote sensing and terrestrial measurements at multiple time points. The most unpredictable component of forest change is disturbance, either natural (e.g., wind throw) or man-made (e.g., harvesting). Temporal gaps between the remote sensing remeasurement window and the terrestrial remeasurement window introduce blind spots for disturbance detection that increase the prevalence and influence of outliers. Moreover, perfect temporal synchronicity is logistically problematic in data collection. In the Swiss NFI, for example, complete national coverage of leaves-on digital stereophotographs is guaranteed only every 6 years, and during that time, the measurements are taken regionally, whereas the annual terrestrial sample is uniformly distributed across the entire country. This leads one to expect a rather low goodness of fit for $\hat{Y}^{(1)}_\Delta(x)$ and $\hat{Y}_\Delta(x)$ under the direct method, which is our motivation for also employing the kNN regression estimator in our case study.

3.3. Indirect estimation

The indirect change estimation method requires static estimates of the forest state at two time points, and the net change is calculated as the difference between the two estimates. We again consider two time points t_1 and t_2 and, without loss of generality, assume that $t_2 > t_1$. Let $s_1(t_k)$ and $s_2(t_k)$ be the first- and second-phase samples of points taken at t_k, respectively. For simplicity, we assume that the points included in the first and second phases are the same, i.e., $s_1 := s_1(t_1) = s_1(t_2)$ and $s_2 := s_2(t_1) = s_2(t_2)$. We consider two potential scenarios for the final phase where the local densities $Y(t_1, x)$ and $Y(t_2, x)$ are observed at the same points in s_3, i.e., $s_{31} = s_{32}$, and where they are observed at completely distinct points, i.e., $s_{31} \cap s_{32} = \emptyset$.

We begin by using eq. 5 to estimate the forest states at t_1 and t_2. Thus we take the same sample points from remote sensing and the same sample points from previous measurements at t_2 and t_1. The three- and two-phase generalized difference estimators of state at time t_k are denoted

$$\hat{Y}_{3p}(t_k) = \frac{1}{n_1}\sum_{x\in s_1}\hat{Y}^{(1)}(t_k, x) + \frac{1}{n_2}\sum_{x\in s_2}(\hat{Y}(t_k, x) - \hat{Y}^{(1)}(t_k, x)) + \frac{1}{n_{3k}}\sum_{x\in s_{3k}}(Y(t_k, x) - \hat{Y}(t_k, x)) \quad (13)$$

$$\hat{Y}_{2p}(t_k) = \frac{1}{n_2}\sum_{x\in s_2}\hat{Y}(t_k, x) + \frac{1}{n_{3k}}\sum_{x\in s_{3k}}(Y(t_k, x) - \hat{Y}(t_k, x)) \quad (14)$$

for $k = 1, 2$, and the estimators of $\Delta_{\bar{Y}}(t_1, t_2)$ are

$$\hat{\Delta}_{\text{indir},3p} = \hat{Y}_{3p}(t_2) - \hat{Y}_{3p}(t_1) \quad (15)$$

$$\hat{\Delta}_{\text{indir},2p} = \hat{Y}_{2p}(t_2) - \hat{Y}_{2p}(t_1)a \quad (16)$$

We can use any model to calculate the predictions, $\hat{Y}^{(1)}(t_k, x)$ and $\hat{Y}(t_k, x)$. Under the external model assumption, $\hat{Y}_{3p}(t_k)$ and $\hat{Y}_{2p}(t_k)$ are design-unbiased estimators of $\bar{Y}(t_k)$, which immediately implies that $\hat{\Delta}_{\text{indir},3p}$ and $\hat{\Delta}_{\text{indir},2p}$ are unbiased estimators of $\Delta_{\bar{Y}}(t_1, t_2)$. The theoretical variances will differ slightly at this point for the two scenarios where $s_{31} = s_{32}$ and $s_{31} \cap s_{32} = \emptyset$. An example derivation is given in Appendix A.

3.3.1. *Scenario one: $s_{31} = s_{32}$*

As $s_{31} = s_{32}$, we can use the simpler notation with s_3 and n_3. The theoretical variances are

$$\mathbb{V}(\hat{\Delta}_{\text{indir},3p}(t_1, t_2)) = \frac{1}{n_1}\mathbb{V}(Y(x, t_2) - Y(x, t_1)) + \left(1 - \frac{n_2}{n_1}\right)\frac{1}{n_2} \times \mathbb{V}\left(R^{(1)}1(x, t_2) - R^{(1)}(x, t_1)\right) + \left(1 - \frac{n_3}{n_2}\right)\frac{1}{n_3}\mathbb{V}(R(x, t_2) - R(x, t_1)) \quad (17)$$

$$\mathbb{V}(\hat{\Delta}_{\text{indir},2p}(t_1, t_2)) = \frac{1}{n_2}\mathbb{V}(Y(x, t_2) - Y(x, t_1)) + \left(1 - \frac{n_3}{n_2}\right)\frac{1}{n_3}\mathbb{V}(R(x, t_2) - R(x, t_1)) \quad (18)$$

Note that in this scenario, the $Y(x, t_2) - Y(x, t_1)$, $R^{(1)}1(x, t_2) - R^{(1)}(x, t_1)$, and $R(x, t_2) - R(x, t_1)$ are all observable because each $x \in s_3$ is observed at both t_1 and t_2. Thus, the external variance estimators are based on sample copies of each variance term in s_3.

3.3.2. *Scenario two: $s_{31} \cap s_{32} = \emptyset$*

The theoretical variances look a little different from eqs. 17 and 18

$$\mathbb{V}(\hat{\Delta}_{\text{indir},3p}(t_1, t_2)) = \frac{1}{n_1}\mathbb{V}(Y(x, t_2) - Y(x, t_1)) + \left(1 - \frac{n_2}{n_1}\right)\frac{1}{n_2}\mathbb{V}\left(R^{(1)}1(x, t_2) - R^{(1)}(x, t_1)\right) + \left(1 - \frac{n_{31}}{n_2}\right)\frac{1}{n_{31}}\mathbb{V}(R(x, t_2)) + \left(1 - \frac{n_{32}}{n_2}\right)\frac{1}{n_{32}}\mathbb{V}(R(x, t_1)) \quad (19)$$

$$\mathbb{V}(\hat{\Delta}_{\text{indir},2p}(t_1, t_2)) = \frac{1}{n_2}\mathbb{V}(Y(x, t_2) - Y(x, t_1)) + \left(1 - \frac{n_{31}}{n_2}\right)\frac{1}{n_{31}}\mathbb{V}(R(x, t_1)) + \left(1 - \frac{n_{32}}{n_2}\right)\frac{1}{n_{32}}\mathbb{V}(R(x, t_2)) \quad (20)$$

Fig. 1. Map of study area in Switzerland with locations of first-phase plots.

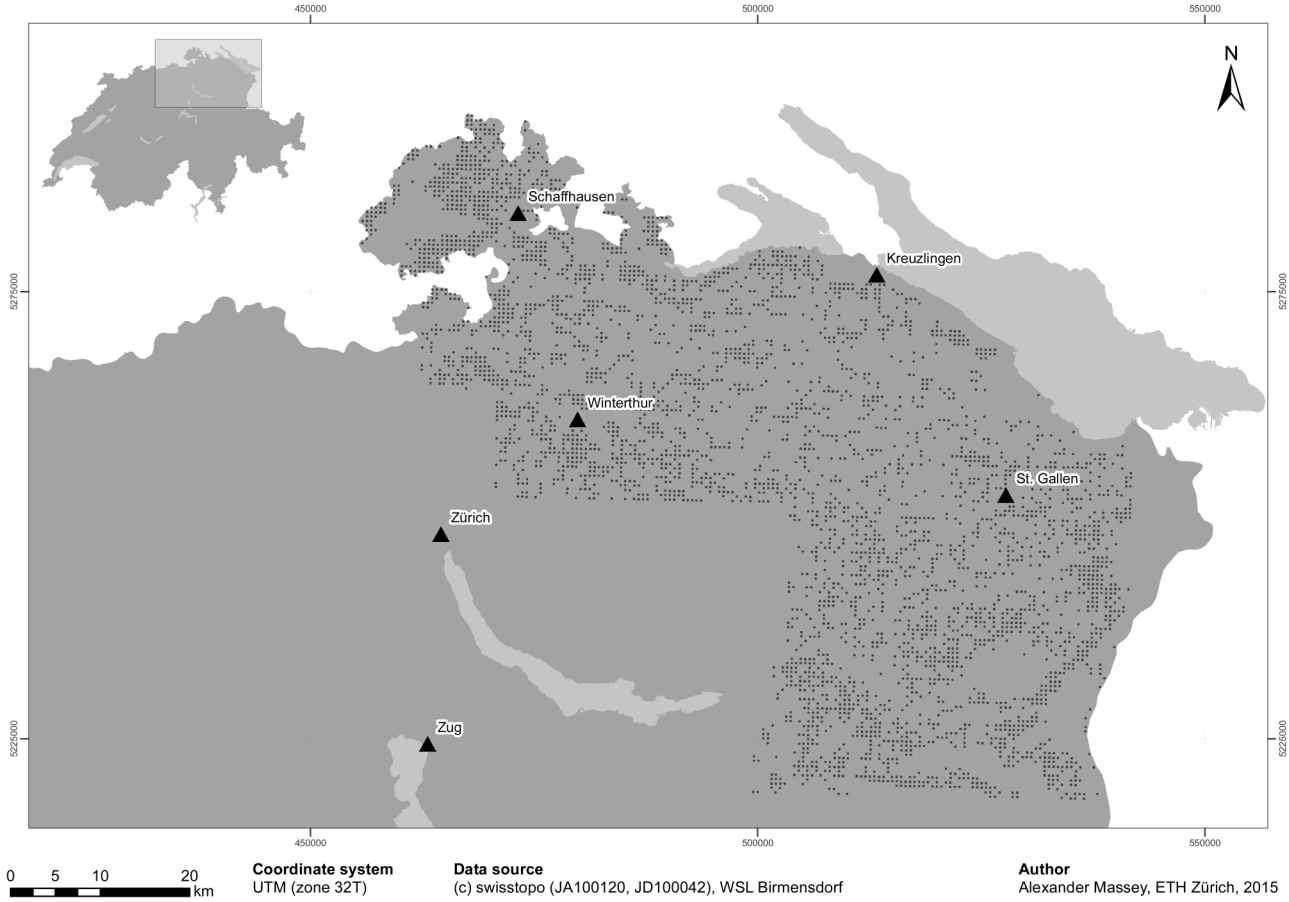

In this scenario, we only need to estimate $\mathbb{V}(R(x, t_1))$ and $\mathbb{V}(R(x, t_2))$ rather than $\mathbb{V}(R(x, t_2) - R(x, t_2))$, because s_{31} is conditionally independent of s_{32}. This can be done using sample copies in s_{31} and s_{32}, respectively. However, the problem is that we still need to estimate $\mathbb{V}(Y(x, t_2) - Y(x, t_1))$ and $\mathbb{V}(R^{(1)}1(x, t_2) - R^{(1)}(x, t_1))$, but there exists no x where $Y(x,t_2) - Y(x,t_1)$ or $R^{(1)}1(x,t_2) - R^{(1)}(x,t_1)$ are observed in the realized sample. We can certainly estimate each variance using the bootstrap to remain firmly in the design-based setup, or we can attempt to construct an analytical variance estimator using an ad hoc solution. To construct such an ad hoc solution for the two-phase estimator, consider the decomposition

$$\mathbb{V}(Y(t_2, x) - Y(t_1, x)) = \mathbb{V}(Y(t_2, x)) + \mathbb{V}(Y(t_1, x)) - 2\rho_{Y_{\Delta t}}\sqrt{\mathbb{V}(Y(t_2, x))\mathbb{V}(Y(t_1, x))} \quad (21)$$

Notice that only the correlation, $\rho_{Y_{\Delta t}}$, is inestimable from the available sample. We emphasize that despite $\rho_{Y_{\Delta t}}$ being unobserved in the realized sample, it certainly is a parameter that exists in the population. It is reasonable to assume that $\rho_{Y_{\Delta t}} \geq 0$, so ignoring the third term completely would unsatisfactorily inflate the variance. A more efficient variance estimate is obtained if one can make a reasonably informed inference about the anticipated correlation between $Y(t_1, x)$ and $Y(t_2, x)$ from past inventories. If such information is available, then one could construct a conservative model-based imputation of $\rho_{Y_{\Delta t}}$ and then apply the design-based variance formula described in eq. 20 using sample copies of every variance term on the right-hand side.

In theory, one could follow a similar procedure to impute $\rho_{R^{(1)}_{\Delta}(x)}$ and estimate $\mathbb{V}(\hat{\Delta}_{\text{indir,3p}}(t_1, t_2))$. However, this may not be reasonable. First of all, the same type of auxiliary information used in the model predictions would have to be available for historical inventories, which might be unlikely considering that technologies in remote sensing tend to change frequently over time. Second, it is not clear that one can assume a lower bound for $\rho_{R^{(1)}_{\Delta}(x)}$ or even that $\rho_{R^{(1)}_{\Delta}(x)} \geq 0$. Imputing a positive $\rho_{R^{(1)}_{\Delta}(x)}$ when it should be negative will actually lead to an underestimation of the variance, which should be avoided.

3.3.3. *Advantages and drawbacks*

With the exception of $\hat{\Delta}_{\text{indir,3p}}(t_1, t_2)$ when $s_{31} \cap s_{32} = \emptyset$, analytical formulations of the variance estimators exist just as for the direct estimators. However, net change can be calculated over any arbitrary time span regardless of the observability of $Y_{\Delta}(x)$, which makes them more flexible. The downside to this flexibility is that one may have to rely on a bootstrap variance to stay purely design based. The proposed ad hoc procedure seems reasonable only for the two-phase estimator and is a bit of a mixture of the design-based and model-dependent philosophies. The other main drawback is that the models are fit to predict state, which leads us to conjecture that there exists at least some degree of suboptimality for predicting change.

4. Case study

4.1. Study area

The study area is located in the northeast corner of Switzerland and draws information from multiple Swiss NFIs, as well as an updated canopy height model derived by stereo-image matching of a digital surface model (DSM) generated by aerial stereo imagery and a previously existing digital terrain model. Figure 1 displays a map. Roughly 48% of the area is in the Swiss Plateau region

where the incidence of man-made intervention is the heaviest, 50% of the area is in the Jura or pre-Alps regions where moderate intervention occurs, and the remaining 2% of the area lies in the Alps region where little man-made disturbance occurs. The target period over which net change is to be estimated occurs between years 2004–2005 and 2010–2011, representing a span of approximately 6 years, on average.

The 3771 first-phase plots are located on a square 500 m × 500 m grid and consist mainly of canopy height information obtained from the DSM. However, for the three-phase indirect estimator, some canopy height information from the manually interpreted stereophotography had to be used to supplement the DSM, which only became available in 2005, because those estimators use the previous inventory plot volume as an auxiliary variable, which works better in conjunction with an aerial disturbance update (Massey et al. (2014)). The second phase consists of 475 plots located on a $\sqrt{2}$ km × $\sqrt{2}$ km subgrid and contains plot volumes from the previous inventory. Note that both inventories preceding the third and fourth Swiss NFIs are periodic and thus summarize a relatively fixed time point. The third phase contains 107 terrestrial plots evaluated under the annual design of the fourth Swiss NFI in 2010 and 2011. As the third NFI in the study area was conducted entirely from 2004 to 2005, we can either choose the third phase such that its plots are remeasured (i.e., $s_{31} = s_{32}$) or such that the none of final phase plots were remeasured (i.e., $s_{31} \cap s_{32} = \emptyset$) without changing the temporal period of our net change estimate. In the latter, $n_{31} = 112$ and $n_{32} = 107$.

4.2. Ground data

On each terrestrial plot, trees are measured using calipers according to two concentric circles measuring 200 m² for trees with diameter at breast height (DBH, 1.3 m) between 12 cm and 36 cm and 500 m² for trees with DBH greater than 36 cm. An approximation of timber volume (over-bark bole volume) is determined by using DBH (via one-way yield table stratified by species) on all eligible trees. For details, we refer the reader to Brassel and Lischke (2001). The first, second, and third Swiss NFIs were periodic and occurred from 1983–1985, 1993–1995, and 2004–2006, respectively. The fourth Swiss NFI, which began in 2009, differs from the first, second, and third NFIs due to the implementation of a new annual design, where one-ninth of the plots are measured every year using interpenetrating grids (≈4.2 km × 4.2 km) to allow for more up-to-date estimates to be available between inventory cycles. At the time of this analysis, data was available from 2009 to 2013 for the fourth Swiss NFI. The Swiss NFI uses permanent plots, and therefore, pairs of plot density estimates can be calculated for any remeasured plot. Further details of the terrestrial data collection of the Swiss NFI can be found in Lanz et al. (2010).

4.3. Digital aerial stereo-photography

4.3.1. Manual interpretation data

As previously mentioned, the first phase of the Swiss NFI consists of a large sample of plots taken from a 500 m × 500 m grid using aerial stereo-photography. The main purpose of these photographs is to make a forest – nonforest decision so that field crews do not have to visit nonforest plots. Photos used for manual interpretation are taken during the leaves-on season and usually occur 2 to 3 years before terrestrial evaluation, which occurs between March and November of each year. In the second and third NFIs, other continuous landscape variables such as canopy height information were also assessed at these plots. The basic sampling unit consists of a 50 m × 50 m square interpretation area, each containing 25 equally spaced raster points arranged in a 5 × 5 design. Note that the canopy height information from this data source was only used in the disturbance correction for the one of the indirect three-phase models because no other data was available. All other canopy height information was derived from the digital canopy height model. Further details about this data, as well as disturbance correction terms, are found in Massey et al. (2014).

4.3.2. Digital canopy height model

A canopy height model with a resolution of 1 m × 1 m was obtained by generating a DSM using ADS40/ADS80 provided by the Swiss Federal Office of Topology (swisstopo) during the leaves-on season and subtracting a previously existing digital terrain model. Comprehensive details about the automated workflow and the stereo-image matching strategy is described in Ginzler and Hobi (2015). All plot-level summary statistics of the canopy characteristics are calculated using 25 m × 25 m interpretation areas centered over the nominal centers of the terrestrial plots. The main statistics of interest were the mean, median, and standard deviation of the canopy heights calculated over a green layer from the topographic map representing forested area. Pixels presumably describing canopy heights outside the range 0 m to 55 m were defined as outliers. Ideally, they should be completely removed, as it is unlikely that the outlying measurement actually describes a canopy height. However, for this data set, they were truncated to either 0 m or 55 m.

The flight plan used to acquire the leaves-on measurements used to calculate the DSM covers different regions each year and takes a maximum of 6 years to get wall-to-wall nationwide coverage. By contrast, the terrestrial Swiss NFI measurements are currently acquired uniformly each year over the entire country. This makes it difficult to obtain good temporal alignment between the canopy height measurements and the terrestrial NFI. The main motivation behind restricting ourselves to the aforementioned study area is to achieve a better temporal alignment between the data sources. Histograms describing the temporal alignment in the study area at t_1 and t_2 are found in Fig. 2. The total absolute deviation of synchronicity describes the sum of the absolute differences between the flight and field dates at t_1 and t_2 in vegetative periods and represents the amount of time where forest disturbance, either natural or manmade, could potentially lead to large discrepancies between the remote sensing prediction and the ground truth.

4.4. Sampling frame

From a sampling perspective, it is best to have a forest versus nonforest decision available before the first-phase sample selection to establish a well-defined sampling frame. However, as no map of forest land exists that conforms perfectly to the official Swiss NFI definition, we use the forest – nonforest decision obtained from manually interpreted aerial photos as opposed to the official decision that is only available for terrestrially measured plots. Although the aerial and terrestrial decisions are made independently, less than 1% of the sampling points have differing classifications. Usually aerial photo interpretation is considered as auxiliary information in a two-phase estimation procedure, but for this case study, it is used primarily to create a working definition of the common forested area between the third and fourth NFIs. Thus all first-, second-, and third-phase plots were classified as nonbush forest by their corresponding manually interpreted aerial photos. It should also be noted that in Switzerland, as in many other European countries, land that is classified as forest cannot become nonforest by legal decision in most cases.

4.5. Target variable

The target variable of interest is the change between times t_1 (i.e., 2004–2005) and t_2 (i.e., 2010–2011) of the growing stock volume ($VOL_\Delta := VOL_{t_2} - VOL_{t_1}$) in cubic meters per hectare ($m^3 \cdot ha^{-1}$) of living trees, excluding shrub forest in the common accessible forest. There is a threshold of 12 cm DBH for trees to be included in the estimates.

Fig. 2. Temporal asynchronicity between digital canopy height model and terrestrial measurements. The total absolute temporal deviation from synchronicity is calculated as the sum over t_1 and t_2 of the absolute value of the flight date of the aerial measurement minus the field date of the terrestrial measurement calculated in vegetative periods.

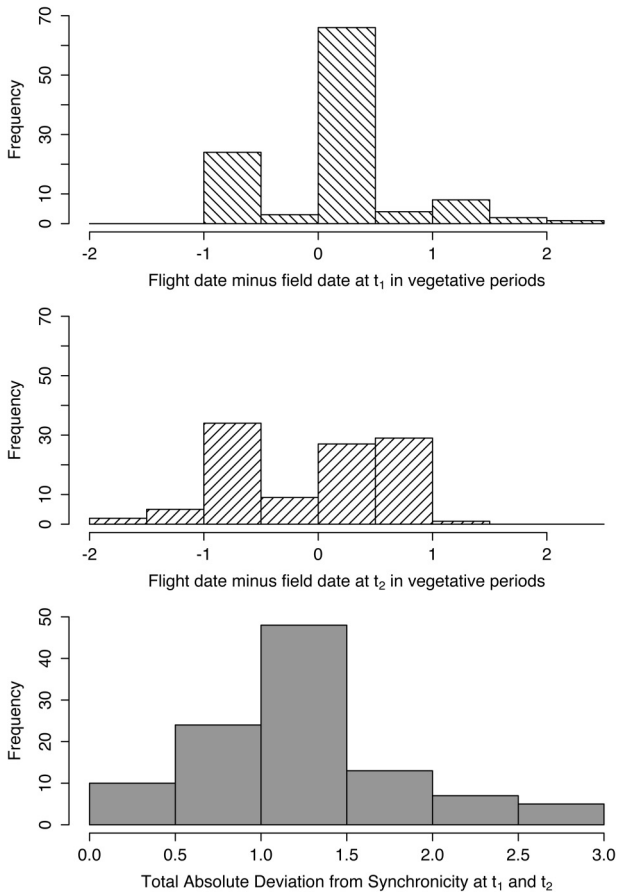

4.6. Auxiliary variables

The main auxiliary variables of interest from remote sensing are derived from the mean canopy height at time t_k (MCH(t_k)), the median canopy height at time t_k (Q50CH(t_k)), and the standard deviation of the canopy height at time t_k (STD(t_k)) calculated over the forested part of the interpretation area. Transformations of these variables were considered, e.g., taking the square and taking the absolute value. For the direct estimators, various parameterizations are available depending whether one includes a single variable for the change between t_1 and t_2 or two separate variables. For example, one may allow MCH(t_1) and MCH(t_2) to be included in the model independently, resulting in two separate coefficients, or one can take a single variable with value MCH(t_2) – MCH(t_1), resulting in a single coefficient. The terrestrial auxiliary variables of interest are derived from previous plot-level measurements of volume and stem count in the second and third NFIs.

4.7. Model selection

The model selection was based on a combination of expert knowledge and an exhaustive variable selection algorithm using Mallows' Cp criterion. Initially, the selection algorithm was used to select models for the two-phase estimators using only remote sensing in the first phase. The three-phase models were chosen such that they include the entire selected two-phase model, as well as a terrestrially derived variable based on the previous measurement and a disturbance correction term. The selected models are displayed in Table 1. For the indirect estimators, the same structure of model variables was kept for each estimate of state at times t_1 and t_2 for simplicity. The same auxiliary variables were used in the *k*NN regression estimators.

Table 1. Auxiliary variables selected for considered models.

Estimator	$\mathbf{Z}^{(1)t}(x)$	$\mathbf{Z}^{(2)t}(x)$
$\hat{\Delta}_{dir,1p}(t_1, t_2)$	…	…
$\hat{\Delta}_{dir,2p}(t_1, t_2)$	$MCH_\Delta(t_1, t_2)$ $STD_\Delta(t_1, t_2)$	…
$\hat{\Delta}_{dir,3p}(t_1, t_2)$	$MCH_\Delta(t_1, t_2)$ $STD_\Delta(t_1, t_2)$	$PREV\_SC_\Delta(t_1, t_2)$
$\hat{\Delta}_{indir,1p}(t_1, t_2)$	…	…
$\hat{\Delta}_{indir,2p}(t_1, t_2)$	$MCH(t_k)$ $(MCH(t_k))^2$ $Q50CH(t_k)$ $(Q50CH(t_k))^2$ $STD(t_k)$	…
$\hat{\Delta}_{indir,3p}(t_1, t_2)$	$MCH(t_k)$ $(MCH(t_k))^2$ $Q50CH(t_k)$ $(Q50CH(t_k))^2$ $STD(t_k)$	$PREV\_VOL(t_k)$ $DIST(t_k)$

Note: The indirect estimator, $\hat{\Delta}_{indir,2p}(t_1, t_2)$, uses the same model variables for $\hat{Y}_{2p}(t_1)$ and $\hat{Y}_{2p}(t_2)$ (likewise for $\hat{\Delta}_{indir,3p}(t_1, t_2)$). The digital canopy height model is used to derive all variables except DIST(t_1), which is based on the change in MCH from the manual interpretation data because the digital canopy height model only began in 2005.

$MCH_\Delta(t_1, t_2) := MCH(t_2) - MCH(t_1)$.

$STD_\Delta(t_1, t_2)$:= absolute value of $STD(t_2) - STD(t_1)$.

$PREV\_SC_\Delta(t_1, t_2)$:= change in stem count from the second to third Swiss NFI.

$MCH(t_k)$:= mean canopy height at time t_k for $k = 1, 2$.

$Q50CH(t_k)$:= median canopy height at time t_k for $k = 1, 2$.

$STD(t_k)$:= standard deviation of canopy height at time t_k for $k = 1, 2$.

$PREV\_VOL(t_k)$:= plot volume from NFI preceding time t_k for $k = 1, 2$.

$DIST(t_k)$:= the disturbance update associated with $PREV\_VOL(t_k)$ corresponding to the change in MCH since the previous inventory.

4.8. Imputing correlation for the fourth Swiss NFI

The ad hoc variance estimator for $\hat{\Delta}_{indir,2p}$ requires correlations to be estimated based on previous inventories. Past data for timber density was taken from all four Swiss NFIs. For every combination of remeasured plots, the number of vegetative cycles between remeasurements is calculated and rounded to the nearest integer. We call this the time lag (denoted LAG), and for each time lag, the sample Pearson correlation coefficient can be calculated. For each of these correlation estimates, a lower bound of a 99% confidence interval can be calculated using Fisher's Z′ transformation.

To make a conservative imputation for $\rho_{Y_{\Delta t}}$, one can model on the lower bound of the 99% confidence interval. The desired model should have an intercept at 1 and converge near to 0 as the years between remeasurements gets larger. This can be obtained by fitting the following linear model and backtransforming the logged response variable with the appropriate bias correction

$$\log(\rho_{Y_{\Delta t}}) = \beta_0 + \beta_1 \mathrm{LAG} + \epsilon \quad (22)$$

Of course, one would not expect the correlation structure over time to be the same across regions with different harvesting intensities. Regions with similar harvesting intensities should be grouped so that sufficient sample size is present for each LAG (for this study, the sample size remained above 80 for each LAG). For

Fig. 3. Correlations by regional grouping. Solid lines represent the linear interpolation of estimated correlations for each time lag (measured in vegetative periods). Time units in terms of vegetative periods is defined as 0.25 for each of the growing season months from May to August and zero for the rest of the year. Dashed lines represent the conservative prediction generated by backtransforming a linear logged response model on the 99% lower bound of the confidence interval.

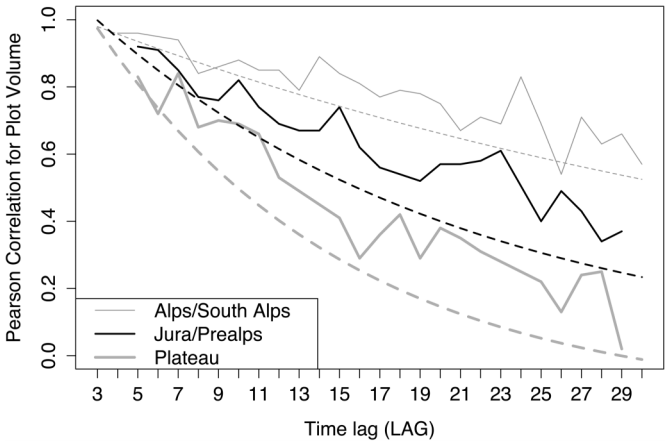

Switzerland, the regional groupings are Jura–pre-Alps, Plateau, and Alps – South Alps. Using the same procedure as described before in each region, one obtains the anticipated correlations presented in Fig. 3. It should be noted that the variance of the point estimates for given years seem to increase with time. This can be compensated for by using weighted least squares weights proportional to either LAG or LAG^2.

4.9. Estimators considered

The two- and three-phase direct and indirect estimators were compared for both scenarios one (i.e., $s_{31} = s_{32}$) and two (i.e., $s_{31} \cap s_{32} = \emptyset$). For each of these estimators and scenarios, both *k*NN and classical linear regression models were tested using the same auxiliary variables. The *k*NN models were fit using the function kknn() from the R package kknn (Schliep and Hechenbichler (2014)). For comparability, only Gaussian kernels were considered, and the choice of *k* was made using leave-one-out cross validation. It should be noted that kknn() automatically scales all auxiliary variables to have equal standard deviations. The classical regression estimators were calculated using lm(), and the bootstrap was calculated using boot() from the R package boot (Canty and Ripley (2015)), which is easily adapted for parallel processing and very computationally efficient. The bootstrap resampling was applied to the first phase only, as described in section 3.2.2. It should be noted that an alternative bootstrap algorithm was also considered adapted from the double sampling bootstrap procedure proposed by Wolter (2007). The Wolter procedure fixes the second- and third-phase sample sizes across all bootstrap samples but is somewhat more involved to implement using the parallel features built into boot(). Because the results from the bootstrap with the Wolter procedure were only negligibly different from the simpler bootstrap described in section 3.2.2, it will not be discussed any further here.

4.10. Results

The estimates with their corresponding standard error estimates are found in Table 2. None of the point estimates are statistically different from each other. As the mean and the classical regression estimators are known to be (asymptotically) unbiased, this indicates some assurance that all estimators are in fact unbiased, even those using the *k*NN model, which possesses less clear

Table 2. Point estimates and standard errors for net change ($m^3 \cdot ha^{-1}$) from 2004–2005 to 2010–2011.

Estimator	Model	Scenario	Estimate	Ext. SE	Boot. SE	*k*	R^2
$\hat{\Delta}_{dir,1p}(t_1, t_2)$	—	One	15.22	11.65	11.54	—	—
$\hat{\Delta}_{dir,2p}(t_1, t_2)$	Reg	One	19.27	8.69	9.54	—	0.46
$\hat{\Delta}_{dir,3p}(t_1, t_2)$	Reg	One	13.09	8.67	8.76	—	0.46, 0.48
$\hat{\Delta}_{dir,2p}(t_1, t_2)$	*k*NN	One	14.40	7.43	9.14	9	—
$\hat{\Delta}_{dir,3p}(t_1, t_2)$	*k*NN	One	13.14	6.82	8.60	9, 5	—
$\hat{\Delta}_{indir,1p}(t_1, t_2)$	—	One	15.22	11.65	11.54	—	—
$\hat{\Delta}_{indir,2p}(t_1, t_2)$	Reg	One	2.73	13.63	12.74	t_1: —	0.37
						t_2: —	0.39
$\hat{\Delta}_{indir,3p}(t_1, t_2)$	Reg	One	–4.74	14.19	16.91	t_1: —	0.37, 0.78
						t_2: —	0.39, 0.92
$\hat{\Delta}_{indir,2p}(t_1, t_2)$	*k*NN	One	4.41	12.88	14.68	t_1: 10	—
						t_2: 7	—
$\hat{\Delta}_{indir,3p}(t_1, t_2)$	*k*NN	One	–1.88	11.33	16.01	t_1: 10, 6	—
						t_2: 7, 5	—
$\hat{\Delta}_{indir,1p}(t_1, t_2)$	—	Two	20.75	38.61	38.51	—	—
$\hat{\Delta}_{indir,2p}(t_1, t_2)$	Reg	Two	15.64	31.09*	32.30	t_1: —	0.28
						t_2: —	0.15
$\hat{\Delta}_{indir,3p}(t_1, t_2)$	Reg	Two	–11.59	—	18.40	t_1: —	0.28, 0.71
						t_2: —	0.15, 0.70
$\hat{\Delta}_{indir,2p}(t_1, t_2)$	*k*NN	Two	11.62	28.03*	31.30	t_1: 10	—
						t_2: 7	—
$\hat{\Delta}_{indir,3p}(t_1, t_2)$	*k*NN	Two	4.29	—	21.30	t_1: 10, 6	—
						t_2: 7, 5	—

Note: Reg, classical regression estimators were calculated; *k*NN, *k*NN regression estimators were calculated using with Gaussian kernels; scenario one, $s_{31} = s_{32}$; scenario two, $s_{31} \cap s_{32} = \emptyset$; Ext. SE, analytical standard errors derived under the external model assumption; Boot SE, bootstrap standard errors with 25 000 replications; *, ad hoc variances using an imputed $\hat{\rho} = 0.67$. No suitable analogy for R^2 was found for *k*NN, which is why it is not reported. The three-phase reg estimators have two linear models and thus two R^2 values.

mathematical results. However, the direct estimator appears to be far more stable than the indirect estimator. The direct estimators (where $s_{31} = s_{32}$) performed far more predictably compared with their indirect counterparts. Two phases are better than one phase, and three phases are slightly better than two phases. The modest improvement over two phases is validated by the fact that the full model had only a slightly better R^2. The analogous indirect estimators, however, got worse when more auxiliary information was included in the models, despite exhibiting values of R^2 that seemed superior at first glance (some of them were as high as 0.92). These R^2 values refer to how well the models predict state and not the target variable net change. It may seem counterintuitive that they actually led to less precise estimates than if no auxiliary information had been observed at all. Table 2 only displays the R^2 values obtained by the linear models, because the classical interpretation of R^2 as the percentage of the variance explained by the model is no longer valid for *k*NN. The indirect estimators in scenario two (where net change on the plot level was never observed) returned to the more intuitive pattern of two phases being better than one phase but worse than three phases but at the cost of significantly higher standard errors. This implies that if net change is observed, then it should be calculated directly, using three phases if possible.

The analytical standard errors derived under the external model assumption appear to be adequate when used with linear models. The external standard errors of the *k*NN estimators were consistently smaller than their bootstrap counterparts, indicating an overall underestimation of their true design-based variance. The underestimation of the classical regression estimators was more negligible in magnitude, which is to be expected considering that they have fewer parameters to estimate. Overall, *k*NN did not seem to offer much of an advantage over classical regression, which might be expected given that the goodness of fit for the

Fig. 4. Plot-level comparison of direct versus indirect residual terms for the two-phase classical regression estimators. Solid circles represent outlying plots where major disturbance went undetected by the direct model. $\hat{R}_{\Delta}(x)$ corresponds to the direct estimator, whereas $\hat{R}(x, t_2) - \hat{R}(x, t_1)$ corresponds to the indirect estimator.

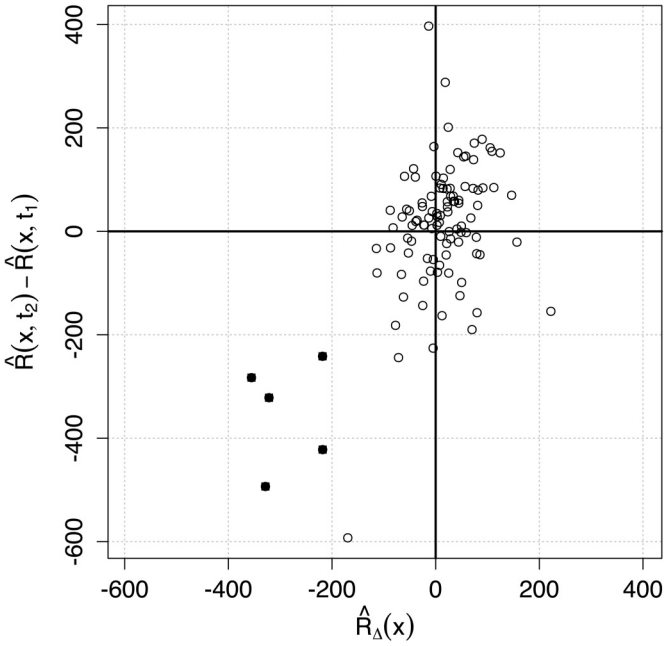

direct models is neither exceptionally low or high (Massey and Mandallaz (2015)). The external variance using the ad hoc method also appears to be adequate, as verified by the bootstrap.

4.11. Discussion

The most disturbing feature of the results is the complete breakdown of the indirect estimator when $s_{31} = s_{32}$ for two and three phases, which did not occur for the direct versions. Consider the two-phase cases. Notice that the first terms in eq. 12 and 18 and all sample sizes are equivalent, so it suffices to examine only the residual variance terms to compare this estimator with the two-phase direct estimator. $\hat{R}(x, t_2) - \hat{R}(x, t_1)$ and $\hat{R}_{\Delta}(x)$ from the classical regression estimators are plotted against each other in Fig. 4. We see that both the direct and indirect estimators performed poorly on many of the same plots and that the effect of these outliers is more pronounced for the indirect method. Overall, the indirect residual terms are more dispersed, which is reasonable considering that the model fit is optimized to predict state rather than change directly. Furthermore, its lack of efficiency seems systematic for outlier and nonoutlier plots. This indicates that if direct estimation is possible, it should be preferred to indirect estimation.

In Fig. 5, the direct model predictions for plot-level change are compared with the ground truth. Plots closer to the dashed line indicate better model predictions. Immediately, it should be obvious that most plots grow modestly and that a small minority of plots experience some kind of dramatic disturbance. The direct model predicted forest disturbance well for all except five plots, marked with solid circles. It should be noted that the direct two-phase model's failure to detect forest disturbances on these five plots resulted in a 33% increase in standard error. Even on a handful of final phase plots, failed disturbance detection can be particularly detrimental to an estimator's precision. As a result, factors contributing to failed disturbance detection must not be ignored, in particular imprecise locations for plot coordinates and temporal asynchronicity between the remote sensing and terrestrial measurements.

Fig. 5. Plot-level predictions versus ground truth for the two-phase direct classical regression estimator. Solid circles represent outlying plots where major disturbance went undetected by the model.

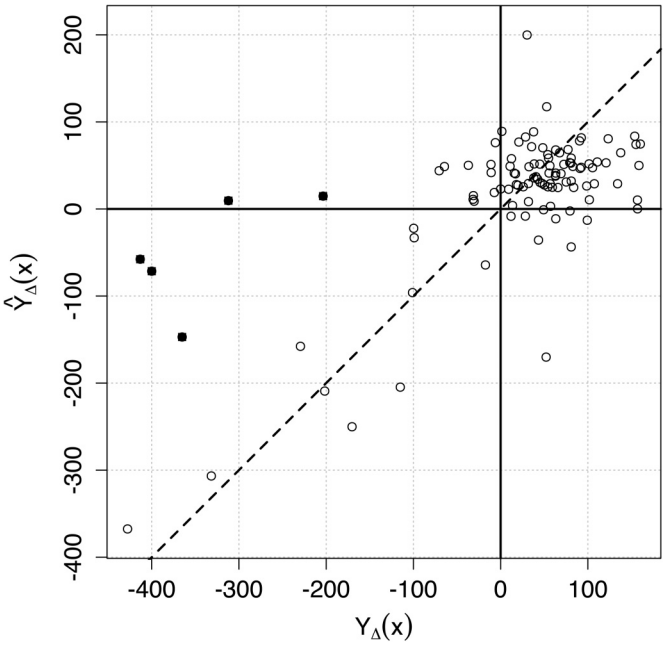

5. Conclusions

Two- and three-phase regression estimation shows promise for improving the precision of net change estimation in the design-based context. If the change is observed on the plot level, the direct method should be employed over the indirect method. The indirect estimators can still be helpful when direct estimation is impossible, which would be the case for inventories with temporary plots or annual designs where the target time period is not a multiple of the remeasurement cycle. The proposed ad hoc procedure for imputing the correlation from previous inventories appears to be a reasonable option for circumventing the issue of not observing plot-level remeasurements, but to remain purely design based, the bootstrap must be used.

For choosing a model, both *k*NN and linear models appear to offer the same magnitudes of precision improvement. However, *k*NN should be used in conjunction with a bootstrap variance estimator where the choice of k and kernel are fixed across all bootstrap samples. The advantage of using linear models via the two- and three-phase classical regression estimators is that the analytical variance estimates derived under the external variance assumption appear to remain valid. The existence of reliable analytical variance estimators allows for simplified implementation and exactly reproducible results. Furthermore, the two- and three-phase estimators can easily be extended to cluster sampling (see Mandallaz (2012, 2013*b*)), which is a common feature in many large-scale forest inventories.

The issue of temporal alignment between remote sensing and terrestrial measurements appears to be of greater importance in change estimation than it is in state estimation, as the failed detection of even a small number of plots with large disturbances has the potential to dramatically inflate the variance. This creates a dilemma for large-scale forest inventories that have operational incentives to collect remote sensing data regionally rather than uniformly across the entire country, because establishing good temporal synchronicity requires harmonizing aerial and terrestrial campaigns.

Acknowledgements

We express our thanks to Christian Ginzler (WSL, Birmensdorf) for his technical assistance with the data processing tasks and to the reviewers for their helpful comments and suggestions.

References

Barklund, A. 2009. The Swedish forestry model. Royal Swedish Academy of Agriculture and Forestry.

Brassel, P., and Lischke, H. 2001. Swiss National Forest Inventory: methods and models of the second assessment. WSL Swiss Federal Research Institute, Birmensdorf, technical report.

Canty, A., and Ripley, B.D. 2015. boot: bootstrap R (S-Plus) functions. R package version 1.3-15.

Ginzler, C., and Hobi, M. 2015. Countrywide stereo-image matching for updating digital surface models in the framework of the Swiss National Forest Inventory. Remote Sens. **7**: 4343–4370. doi:10.3390/rs70404343.

Haara, A., and Kangas, A. 2012. Comparing K nearest neighbours methods and linear regression — is there reason to select one over the other? Mathematical and Computational Forestry And Natural-Resource Sciences, **4**: 50–65.

Lanz, A., Brändli, U.-B., Brassel, P., Ginzler, C., Kaufmann, E., and Thrürig, E. 2010. Switzerland. *In* National Forest Inventories Pathways for Common Reporting. Chapter 36. *Edited by* E. Tomppo, T. Gschwantner, M. Lawrence, R. McRoberts, and Winzeler. Springer. pp. 555–565.

Lüpke, N., Hansen, J., and Saborowski, J. 2012. A three-phase sampling procedure for continuous forest inventory with partial remeasurement and updating of terrestrial sample plots. Eur. J. For. Res. **131**: 1979–1990. doi:10.1007/s10342-012-0648-z.

Mandallaz, D. 2008. Sampling techniques for forest inventories. Chapman and Hall, Boca Raton, Florida.

Mandallaz, D. 2012. Design-based properties of small-area estimators in forest inventory with two phase sampling. ETH Zurich, Department of Environmental Systems Science, technical report. Available from http://e-collection.library.ethz.ch.

Mandallaz, D. 2013*a*. New regression estimators in forest inventories with two-phase sampling and partially exhaustive information: a design-based Monte Carlo approach with applications to small-area estimation. Can. J. For. Res. **43**(11): 1023–1031. doi:10.1139/cjfr-2013-0181.

Mandallaz, D. 2013*b*. Regression estimators in forest inventories with three-phase sampling and two multivariate components of auxiliary information. ETH Zurich, Department of Environmental Systems Science, technical report. Available from http://e-collection.library.ethz.ch.

Mandallaz, D. 2014. A three-phase sampling version of the generalized regression estimator with partially exhaustive information. Can. J. For. Res. **44**(4): 383–388. doi:10.1139/cjfr-2013-0449.

Massey, A., and Mandallaz, D. 2015. Comparison of classical, kernel-based and nearest neighbors regression estimators using the design-based Monte Carlo approach for two-phase forest inventories. Can. J. For. Res. **42**(11): 1480–1488. doi:10.1139/cjfr-2015-0151.

Massey, A., Mandallaz, D., and Lanz, A. 2014. Integrating remote sensing and past inventory data under the new annual design of the Swiss National Forest Inventory using three-phase design-based regression estimation. Can. J. For. Res. **44**(10): 1177–1186. doi:10.1139/cjfr-2014-0152.

McRoberts, R., Næsset, E., Gobakkenb, T., and Bollandsås, O.M. 2015. Indirect and direct estimation of forest biomass change using forest inventory and airborne laser scanning data. Remote Sens. Environ. **164**: 36–42. doi:10.1016/j.rse.2015.02.018.

Næsset, E., Bollandsås, O.M., Gobakken, T., Gregoire, T.G., and Ståhl, G. 2013. Model-assisted estimation of change in forest biomass over an 11 year period in a sample survey supported by airborne LiDAR: a case study with post-stratification to provide activity data. Remote Sens. Environ. **128**: 299–314. doi:10.1016/j.rse.2012.10.008.

Särndal, C., Swenson, B., and Wretman, J. 2003. Model assisted survey sampling. Springer Series in Statistics, New York.

Schliep, K., and Hechenbichler, K. 2014. kknn: weighted k-nearest neighbors. R package. version 1.2-5. Available from http://CRAN.R-project.org/package=kknn.

Schreuder, H., Lin, J., and Teply, J. 2000. Annual design-based estimation for the annualized inventories of forest inventory and analysis: sample size determination. USDA Forest Service, Rocky Mountain Research Station, Ogden, Utah, Technical Report RMRS-GTR-66.

Skowronski, N., Clark, K.L., Gallagher, M., Birdsey, R.A., and Hom, J.L. 2014. Airborne laser scanner-assisted estimation of aboveground biomass change in a temperate oak–pine forest. Remote Sens. Environ. **151**: 166–174. doi:10.1016/j.rse.2013.12.015.

Tomppo, E. 2006. The Finnish National Forest Inventory. *In* Proceedings of the 8th Annual Forest Inventory and Analysis Symposium, Monterey, California, October 16–19, 2006. *Edited by* R.E. McRoberts, G.A. Reams, P.C. Van Deusen, and W.H. McWilliams. USDA Forest Service, General Technical Report WO-79. pp. 39–46.

Vidal, C., Bélouard, T., Hervé, J.-C., Robert, N., and Wolsack, J. 2005. The Finnish National Forest Inventory. *In* Proceedings of the 7th Annual Forest Inventory and Analysis Symposium, Portland, Maine, 3–6 October, 2005. *Edited by* R.E. McRoberts, G.A. Reams, P.C. Van Deusen, and W.H. McWilliams. USDA Forest Service, General Technical Report WO-77. pp. 67–73.

Wolter, K. 2007. Introduction to variance estimation. 2nd edition. Springer Science and Business Media, New York.

Appendix A

We now give an example of the derivation of one of the indirect net change estimators, $\hat{\Delta}_{\text{indir,2p}}$, as an outline of the technique by which the theoretical expectation and variances of all the indirect estimators can be derived. For this example, only scenario two is considered, which means that we assume that s_2 consists of the same sample of points at t_1 and t_2, $s_{31} \cap s_{32} = \emptyset$, and $t_1 < t_2$. Recall that s_2 is the result of uniform independent sampling from F and s_{3k} is SRS without replacement from s_2. Working under the external model assumption, we want to demonstrate the two following results:

$$\mathbb{E}_{2,3}(\hat{\Delta}_{\text{indir,2p}}) = \mathbb{E}(\hat{Y}_{2p}(t_2)) - \mathbb{E}(\hat{Y}_{2p}(t_1)) = \overline{Y}(t_2) - \overline{Y}(t_1)$$

$$\mathbb{V}_{2,3}(\hat{\Delta}_{\text{indir,2p}}) = \frac{1}{n_2}\mathbb{V}(Y(t_2,x) - Y(t_1,x)) + \left(1 - \frac{n_{31}}{n_2}\right)\frac{1}{n_{31}}\mathbb{V}(R(t_1,x)) + \left(1 - \frac{n_{32}}{n_2}\right)\frac{1}{n_{32}}\mathbb{V}(R(t_2,x))$$

For the first result, it suffices to show that $\mathbb{E}(\hat{Y}_{2p}(t_k)) = \overline{Y}(t_k)$ for $k \in 1, 2$.

$$\begin{aligned}\mathbb{E}_{2,3}(\hat{Y}_{2p}(t_k)) &= \mathbb{E}_2\mathbb{E}_{3|2}(\hat{Y}_{2p}(t_k)) \\ &= \mathbb{E}_2\left(\frac{1}{n_2}\sum_{x\in s_2}\hat{Y}(x) + \mathbb{E}_{3|2}\left(\frac{1}{n_{3k}}\sum_{x\in s_{3k}}(Y(x) - \hat{Y}(x))\right)\right) \\ &= \mathbb{E}_2\left(\frac{1}{n_2}\sum_{x\in s_2}\hat{Y}(x)\right) + \mathbb{E}_2\left(\frac{1}{n_2}\sum_{x\in s_2}Y(x)\right) - \mathbb{E}_2\left(\frac{1}{n_2}\sum_{x\in s_2}\hat{Y}(x)\right) \\ &= \overline{Y}(t_k)\end{aligned}$$

So $\hat{\Delta}_{\text{indir,2p}}$ is exactly unbiased under the external model assumption. For the theoretical variance, we will use the decomposition $\mathbb{V}_{2,3}(\hat{\Delta}_{\text{indir,2p}}) = \mathbb{V}_2(\mathbb{E}_{3|2}(\hat{\Delta}_{\text{indir,2p}})) + \mathbb{E}_2(\mathbb{V}_{3|2}(\hat{\Delta}_{\text{indir,2p}}))$. For the first term, we get

$$\begin{aligned}\mathbb{V}_2(\mathbb{E}_{3|2}(\hat{\Delta}_{\text{indir,2p}})) &= \mathbb{V}_2\left(\frac{1}{n_2}\sum_{x\in s_2}Y(t_2,x) - \frac{1}{n_2}\sum_{x\in s_2}Y(t_1,x)\right) \\ &= \frac{1}{n_2}\mathbb{V}(Y(t_2,x) - Y(t_1,x))\end{aligned}$$

The subscripted 2 in the variance and expectation is shorthand emphasizing the sampling procedure generating the first phase in F and is dropped for notational simplicity in the final result. For the second term, we get

$$\begin{aligned}\mathbb{E}_2(\mathbb{V}_{3|2}(\hat{\Delta}_{\text{indir,2p}})) &= \mathbb{E}_2\left(\mathbb{V}_{3|2}\left(\frac{1}{n_2}\sum_{x\in s_2}(\hat{Y}(t_2,x) - \hat{Y}(t_1,x)) + \frac{1}{n_{32}}\sum_{x\in s_{32}}R(t_2,x) - \frac{1}{n_{31}}\sum_{x\in s_{31}}R(t_1,x)\right)\right) \\ &= \mathbb{E}_2\left(\mathbb{V}_{3|2}\left(\frac{1}{n_{32}}\sum_{x\in s_{32}}R(t_2,x)\right)\right) + \mathbb{E}_2\left(\mathbb{V}_{3|2}\left(\frac{1}{n_{31}}\sum_{x\in s_{31}}R(t_1,x)\right)\right) \\ &= \left(1 - \frac{n_{31}}{n_2}\right)\frac{1}{n_{31}}\mathbb{V}(R(t_1,x)) + \left(1 - \frac{n_{32}}{n_2}\right)\frac{1}{n_{32}}\mathbb{V}(R(t_2,x))\end{aligned}$$